Theory of water and charged liquid bridges

K. Morawetz
Münster University of Applied Science, Stegerwaldstrasse 39, 48565 Steinfurt, Germany
International Institute of Physics (IIP), Avenida Odilon Gomes de Lima 1722, 59078-400 Natal, Brazil and
Max-Planck-Institute for the Physics of Complex Systems, 01187 Dresden, Germany
(Received 3 July 2011; published 2 August 2012)

The phenomenon of liquid bridge formation due to an applied electric field is investigated. A solution of a charged catenary is presented, which allows one to determine the static and dynamical stability conditions where charged liquid bridges are possible. The creeping height, the bridge radius and length, as well as the shape of the bridge are calculated showing an asymmetric profile, in agreement with observations. The flow profile is calculated from the Navier-Stokes equation leading to a mean velocity, which combines charge transport with neutral mass flow and which describes recent experiments on water bridges.

DOI: 10.1103/PhysRevE.86.026302 PACS number(s): 47.57.jd, 47.65.−d, 83.80.Gv, 05.60.Cd

I. INTRODUCTION

A. The phenomenon

The formation of a water bridge between two beakers under high voltage is a phenomenon known for over 100 years [1]. When two vessels are brought into close contact and a high electric field is applied between the vessels, the water starts creeping up the beakers and forms a bridge which is maintained over a certain distance, as schematically illustrated in Fig. 1. Due to the voltage applied by the vessels, the electric field is longitudinally oriented inside the cylindrical bridge. This has remained an attractive phenomenon in current experimental activities [2,3]. On one hand, the properties of water are so complex that a complete microscopic theory of this effect is still lacking. On the other hand, the formation of water bridges on nanoscales is of interest both for a fundamental understanding of electrohydrodynamics and for applications ranging from atomic force microscopy [4] to electrowetting problems [5]. Microscopically, the nanoscale wetting is important to confine chemical reactions [6], which reveals an interesting interplay between field-induced polarization, surface tension, and condensation [7,8].

Molecular dynamical simulations have been performed in order to explore the mechanism of water bridges at the molecular level, leading to the formation of aligned dipolar filaments between the boundaries of nanoscale confinements [9]. A competition was found between the orientation of molecular dipoles and the electric field, leading to a threshold where the rise of a pillar overcomes the surface tension [8]. In this respect, the understanding of the microscopic structure is essential to explain such phenomena in microfluidics [10]. The problem is connected with the dynamics of charged liquids, which is important for capillary jets [11], current applications in ink printers, and electrosprays [12,13]. Consequently, the nonlinear dynamics of the breakup of free surfaces and flows has been studied intensively [14,15].

Much physical insight can be gained already on the macroscopic scale, where the phenomenon of liquid bridging is not restricted to water but can be observed in other liquids too [16], which shows that it has its origin in electrohydrodynamics [17] rather than in molecular-specific structures. The traditional treatment is based on the Maxwell pressure tensor where the electric field effects comes from the ponderomotoric forces and are due to the boundary conditions of electrodynamics [18]. This is based exclusively on the fact that bulk-charge states decay on a time scale of the dielectric constant divided by the conductivity, $\epsilon\epsilon_0/\sigma$, which for pure water takes 0.14 ms. This decay time of bulk charges follows from the continuity of charge density $\dot{\rho}_c = -\nabla\cdot\mathbf{j}$ combined with Ohm's law $\mathbf{j} = \sigma\mathbf{E} = -\sigma\nabla\phi$, where the source of the electric field is given by the potential $\nabla^2\phi = -\rho_c/\epsilon\epsilon_0$. An overview of the different forces occurring in microelectrode structures is given in Ref. [19].

This simple Ohm picture leads to a problem in partially charged liquids. Following the Ohm picture, one has a constant velocity or current density of charged particles caused by the external field and limited by friction. In contrast, for incompressible fluids, the total mass flux cannot be constant but is dependent on the area where it is forced to flow through. Both pictures seem to be impossible to reconcile. In this paper, we will present a discussion of this seeming contradiction, leading to a dynamical stability criterion for the water bridge and a combined flow expression. This is in line with the idea of Ref. [17], where the bulk charges have been assumed to be realized in a surface sheet. While there the migration of charges to the surface has been considered to form a charged surface sheet, we adopt here the viewpoint of homogeneously distributed bulk charges which flow in the field direction rather than forming a surface sheet.

In the absence of bulk charges, the forces on the water stream are caused by the pressure due to the polarizability of water described by the high dielectric susceptibility ϵ. This pressure leads to the catenary form of the water bridge, such as a hanging chain [20]. While the simplified model of Ref. [16] employing a capacitor picture already leads to a critical field strength for the formation of the water bridge, the catenary model [20] has not been reported to yield such a critical field. In this paper, we will show that even the uncharged catenary provides indeed a minimal critical field strength for the water bridge formation in dependence on the length of the bridge. This critical field strength is modified if charges are present in the bridge, which we will discuss here with the help of a charged catenary solution. This allows us to explain the asymmetry found in the bridge profile [3].

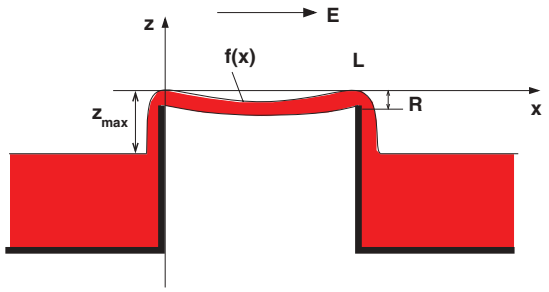

FIG. 1. (Color online) The schematic picture of a water bridge between two beakers.

B. Overview

The scenario of water or other dielectric bridges is understood as follows. Applying an electric field parallel to two attached vessels, the water creeps up the beaker and forms a bridge, as is nicely observed and pictured in Ref. [2]. This bridge can be elongated up to a critical field strength and forms a catenary, which becomes asymmetric for higher gravitation to electric field ratios [3]. The critical value for stability is sensitively dependent on ion concentrations breaking off already at very low concentrations. The amount of mass flow through the bridge does not follow simple Ohmic transport, as we will see in this paper. The schematic picture of the water bridge is given in Fig. 1.

In this paper, we want to advocate the following picture. Imaging a snapshot of the charges flowing through the bridge, we cannot decide whether the observed charges are due to static bulk charges or to the floating motion of Ohmic bulk charges. We can associate this flow of charges within the liquid bridge with a dynamical bulk charge in the mass motion, which is not covered by the decay of Ohmic bulk charges discussed above. Such a picture is supported by the experimental observation of possible copper ion motion [21] and by the observation that the water bridge is highly sensitive to additional external electric fields [22]. Strong fields even create small cone jets [2]. This dynamical bulk charge will lead us to the necessity to solve the catenary problem including bulk charges. Though charged membranes have been discussed in the literature [23], the analytical solution of the charged catenary is offered in this paper.

The picture of Ohmic resistors and capacitors as described above is not sufficient, as one can see from the observation that adding a small amount of electrolytes to the clean water destroys the water bridge almost immediately. In other words, good conducting liquids should not form a water bridge. We will derive an upper bound for charges possibly carried in water in order to remain in stable liquid bridges. Though we present all calculations for the water parameters summarized in Table I, the theory applies as well to any dielectric liquid in electric fields.

Four theoretical questions have to be answered: (i) How is the electric field influencing the height $z_{\max}$ in which water can creep up? (ii) What is the radius $R(x)$ along the bridge? (iii) What is the form $z = f(x)$ of the water bridge, and what are the static constraints on the bridge? (iv) Which dynamical constraints can be found for possible bridge formation?

TABLE I. Variables and parameters used within this paper for water.

Density	$\rho = 10^3$ kg/m^3
Dielectric susceptibility	$\epsilon = 81$
Surface tension	$\sigma_s = 7.27 \times 10^{-2}$ N/m
Viscosity	$\eta = 1.5 \times 10^{-3}$ Ns/m^2
Conductivity of clean water	$\sigma_0 = 5 \times 10^{-6}$ A/Vm
Molecular conductivity of NaCl	$\lambda = 12.6 \times 10^{-3}$ Am^2/Vmol
Heat capacity	$c_p = 4.187$ J/gK

We will address all four questions with the help of four parameters composed of the properties of water summarized in Table I. The first one is the capillary height,

$$a = \sqrt{\frac{2\sigma_s}{\rho g}} = 3.8 \text{ mm}, \tag{1}$$

with surface tension σ_s, particle density ρ, and gravitational acceleration g. The second parameter is the water column height balancing the dielectric pressure, called creeping height,

$$b(E) = \frac{\epsilon_0(\epsilon - 1)E^2}{\rho g} = 7.22\bar{E}^2 \text{ cm}, \tag{2}$$

where the dimensionless electric field $\bar{E}$ is in units of 10^4 V/cm. The third one is the dimensionless ratio of the force density on the charges by the field to the gravitational force density,

$$c(\rho_c, E) = \frac{\rho_c E}{\rho g} = 15.97\bar{E}\bar{\rho}_c, \tag{3}$$

where the charge density $\bar{\rho}_c$ is in units of ng/l. For dynamical consideration, the characteristic velocity

$$u_0 = \frac{\rho g a^2}{32\eta} \approx 3.02 \text{ m/s} \tag{4}$$

will be useful as the fourth parameter.

The outline of the paper is as follows. In the next section, we briefly repeat the standard treatment of creeping height and bubble radius of a liquid, but add the pressure by the external electric field on the dielectric liquid. Then, in Sec. III, we present the form of the bridge in terms of a solution of the catenary equation due to bulk charges. In Sec. IV, we present the flow calculation proposing the picture of moving charged particles due to the field which drag the neutral particles. This will lead to a dynamical stability criterion. Then we compare with the experimental data and show the superiority of the present treatment. A summary and conclusion finishes the discussion in Sec. V.

II. CREEPING HEIGHT AND RADIUS OF BRIDGE

We start to calculate the possible creeping height and use the pressure tensor for dielectric media [18],

$$\sigma^{ik} = -p\delta_{ik} - \sigma_s\left(\frac{1}{R_1} + \frac{1}{R_2}\right) + \epsilon\epsilon_0 E_i E_k - \frac{1}{2}\tilde{\epsilon}\epsilon_0 E^2\delta_{ik}, \tag{5}$$

where p is the pressure in the system, and R_1, R_2 are the principal radii of curvature such that the second term on the right-hand side describes the contribution due to surface tension and the last terms are the parts due to the forces in the dielectric medium. We assume a density-homogeneous liquid such that for the dielectric susceptibility, $\tilde{\epsilon} = \epsilon - \rho(d\epsilon/d\rho)_T \approx \epsilon$. Further, we consider first the stationary problem, which means that viscous forces can be neglected in Eq. (5).

Denoting the components of the normal vector by e^k, the stability condition between water (W) and air (A) is given by

$$\sigma^{ik}_{(A)} e^k_{(A)} = -\sigma^{ik}_{(W)} e^k_{(W)} = -\sigma^{ik}_{(A)} e^k_{(W)}. \tag{6}$$

Since the principal curvature of the tube is much larger radially than parallel, we have $R_2 \sim \infty$, and denoting the coordinate in the direction of the height with z, the pressure difference between water and air is $p_W - p_A = \rho g z$. We employ the boundary conditions for the normal E^n and tangential E^t components of the electric field,

$$E^n_{(A)} = \epsilon E^n_{(W)} = \epsilon E_n, \quad E^t_{(A)} = E^t_{(W)} = E_t, \tag{7}$$

and the balance (6) with (5) reads

$$\rho g z + \frac{\sigma_s}{R_1} = \frac{1}{2}\epsilon_0(\epsilon - 1)\left(\epsilon E_n^2 + E_t^2\right). \tag{8}$$

Please note that due to the migration of charges to the surface, one should consider a surface charge here in principle. We adopt throughout the paper the simplified picture that the charges remain bulklike due to the preferred motion along the field and no surface charges are formed. The influence of such surface charges is considered as marginal since the curvature of the bridge is minimal, leading to preferential tangential components of electric fields.

We assume the electric field in the x direction such that $E_t = -E\cos\alpha$, $E_n = E\sin\alpha$, where $z'(x) = \tan\alpha$ is the increase of the surface line of the water, as illustrated in Fig. 2. Using the parameters (1) and (2), we obtain from the stability condition (8) the differential equation

$$2z - a^2 \frac{z''}{(1+z'^2)^{3/2}} = \frac{\epsilon_0(\epsilon-1)}{\rho g}\left(\epsilon E_n^2 + E_t^2\right) \approx b, \tag{9}$$

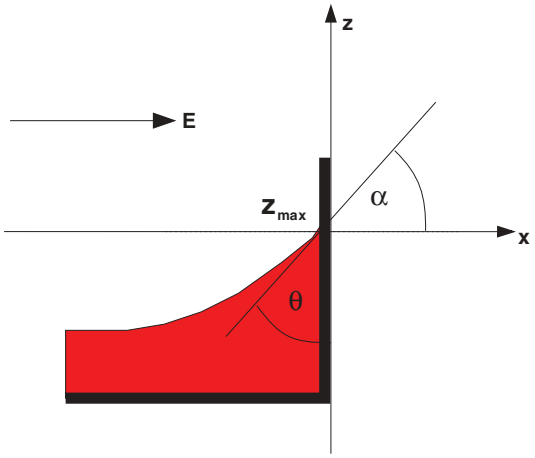

FIG. 2. (Color online) The schematic picture of a water bridge creeping up the vessel due to the applied electric field.

where we used the approximation of small normal electric fields, which is justified if there are no surface charges. This shows the modification of the standard treatment of capillary height by the applied field condensed on the right-hand side. The first integral of Eq. (9) is

$$\frac{z^2}{a^2} + \frac{1}{\sqrt{1+z'^2}} - \frac{bz}{a^2} = 1, \tag{10}$$

and we have used the condition that for $x \to \infty$, the surface is $z = z' = 0$. The explicit solution of the surface curve $z(x)$ is quite lengthy and not necessary here. Instead, we can give directly the maximally reachable height in dependence on the electric field. Therefore, we use the angle $\theta = 90 - \alpha$ of the liquid surface with the wall such that $z'(x) = -\cot\theta$, and from Eq. (10), we obtain

$$z = \frac{b}{2} + \sqrt{\frac{b^2}{4} + a^2(1-\sin\theta)} \leqslant \frac{b}{2} + \sqrt{\frac{b^2}{4} + a^2} = z_{\max}, \tag{11}$$

which shows that without the electric field, the maximal creeping height is just the capillary length (1), as is well known. The other extreme of very high fields leads to the field-dependent length (2), which justifies the name creeping height. This answers the first question concerning creep heights.

The second question, i.e., how large is the radius of the bridge, is answered by equating the pressure due to surface tension with the gravitational force density,

$$\frac{\sigma_s}{R} = \rho g z \approx \rho g 2R, \tag{12}$$

such that the radius of the water bridge is at the beaker,

$$R \approx a/2. \tag{13}$$

Without using this approximation, we could express the curvature again by differential expressions in $z(x)$ defining a radial profile, as can be found in the literature [18]. The radius of the bridge at the beaker is nearly independent of the applied electric field and only depends on the surface tension and gravitational force. Along the bridge, the radius will change with the applied electric field, as we will see later in Sec. IV C.

III. LIQUID BRIDGE SHAPE

A. Charged catenary

Now we turn to the question of which form the water bridge will take. Therefore, we consider the center-of-mass line of the bridge described by $z = f(x)$ with the ends at $f(0) = f(L) = 0$. The force densities are multiplied with the area and the length element $ds = \sqrt{1+f'^2}dx$ to form the free energy. We have the gravitational force density $\rho g f$ and the volume tension $\rho g b$, as well as the force density by dynamical charges $\rho_c E x$ that contributes. The surface tension is negligible here. The form of the bridge will then be determined by the extreme value of the free energy,

$$\int_0^L \mathcal{F}(x)dx = \rho g \int_0^L [f(x) + b - cx]\sqrt{1+f'^2}dx \to \text{extr}, \tag{14}$$

where c is given by Eq. (3) and b is defined in Eq. (2).

As shown in [24] and briefly outlined in the Appendix, the solution can be represented parametrically as

$$f(t)=\frac{1}{1+c^2}\left\{ct+\xi\left[\cosh\left(\frac{t}{\xi}-\frac{Ld}{2\xi}\right)-\cosh\left(\frac{Ld}{2\xi}\right)\right]\right\},$$
$$x(t)=t-cf(t),\quad t\in(0,L), \tag{15}$$

with

$$d=2\frac{\xi}{L}\operatorname{arcosh}\frac{b}{\xi} \tag{16}$$

and ξ as the solution of the equation

$$c=c_m(\xi,b), \tag{17}$$
$$c_m(\xi,b)=-\frac{2\xi}{L}\sinh\frac{L}{2\xi}\left(\frac{b}{\xi}\sinh\frac{L}{2\xi}-\sqrt{\frac{b^2}{\xi^2}-1}\cosh\frac{L}{2\xi}\right).$$

B. Static stability criteria

Without dynamical bulk charges, $c=0$, $d=1$, the solution (15) is just the well-known catenary [20]. The boundary condition (17) reads, in this case,

$$\frac{2b}{L}=\frac{2\xi}{L}\cosh\frac{L}{2\xi}\geqslant\xi_c=1.5088\ldots, \tag{18}$$

which means that without bulk charges, the condition for a stable bridge is

$$b>\frac{1}{2}L\xi_c. \tag{19}$$

Together with Eq. (2), this condition provides a lower bound for the electric field in order to enable a bridge of length L. This lower bound for an applied field clearly appears already for the standard catenary and has not been discussed so far.

Let us now return to the more involved case of bulk charges and the solution of charged catenary (15). The field-dependent lower bound condition (17) is plotted in Fig. 3. One can see that in order to complete (17), the bulk charge parameter c has to be lower than the maximal value of c_m at some ξ_0,

$$c\leqslant c_m(\xi_0,b), \tag{20}$$

which is plotted in the inset of Fig. 3. Remembering the definition of the bulk charge parameter (3), we see that (20) sets an upper bound for the bulk charge in dependence on the electric field. The lower bound (19) of the electric field for the case of no bulk charges is obeyed as well, since the curve in the inset of Fig. 3 starts at $b>L\xi_c/2$, which is the lower bound already present for uncharged catenaries (19).

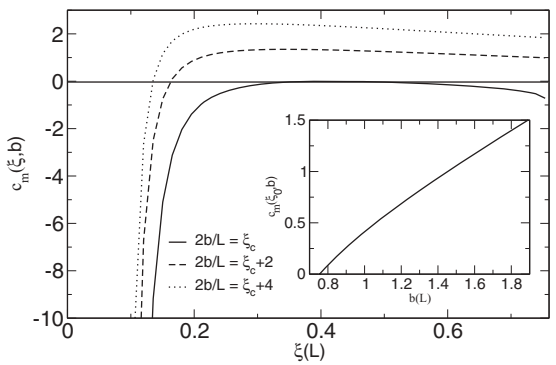

FIG. 3. The upper critical bound for the parameter c according to Eq. (17). The inset shows the maximum in dependence on the creeping parameter b.

This completes the third question concerning the static stability of the bridge. We have found a catenary solution even for bulk charges in the bridge.

IV. DYNAMICAL CONSIDERATION

A. Mass flow of the bridge

We consider now the actual motion of the liquid in the bridge. Here we propose that possible charges in the water will move according to the applied electric field and will drag water particles such that a mean mass motion starts. Due to the low Reynolds numbers (40–100) for water, we can consider the motion as laminar and we can neglect the convection term $\mathbf{u}\nabla\mathbf{u}$ in the Navier-Stokes equation [25], which reads then, for the stationary case,

$$\eta\nabla^2\mathbf{u}-\nabla p+\rho_c\mathbf{E}=0. \tag{21}$$

The gradient of the electric pressure (8) can be given in the direction of the bridge by

$$-\nabla p=\frac{\epsilon_0(\epsilon-1)E^2}{2L}=\frac{b}{2L}\rho g. \tag{22}$$

Here we can adopt the stationary pressure since the viscous pressure is accounted for by the Navier-Stokes equation. Assuming that the flow in the bridge has only a transverse component which is radial dependent, $u(r)$, we can write the Navier-Stokes equation (21) as

$$\frac{\eta}{\rho g}\frac{d}{dr}\left(r\frac{du}{dr}\right)+r\left(\frac{b}{2L}+c\right)=0, \tag{23}$$

with the resulting velocity profile in the direction of the bridge,

$$u(r)-u(R)=2u_0\left(\frac{b}{2L}+c\right)\left(1-\frac{r^2}{R^2}\right), \tag{24}$$

where R is the radius of the bridge and we have introduced the characteristic velocity (4). Please note that we keep the undetermined velocity at the surface of the bridge, $u(R)$. We will assume in the following that it is negligible. The resulting profile (24) has the form of a Poiseuille flow, but with an interplay between forces due to bulk charges and dielectric pressure in relation to gravity.

The mean current relative to the surface motion is easily calculated,

$$I=2\pi\rho\int_0^R drr[u(r)-u(R)]\equiv\rho v\pi R^2, \tag{25}$$

providing the mean velocity of the bridge from Eq. (24) as

$$v=u_0\left(\frac{b}{2L}+c\right). \tag{26}$$

One sees that the ratio of the field-dependent creeping height (2) to the bridge length determines the mean velocity together with possible dynamical bulk charges described by Eq. (3). Since we presently do not have good control over the surface velocity $u(R)$, we approximate it in the following as zero.

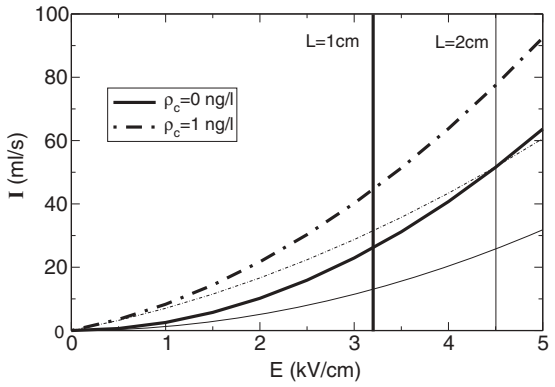

FIG. 4. The mean mass current through the bridge in dependence on the electric field and for two different bulk charge densities. The thick lines are for a bridge length of 1 cm and the thin lines for the corresponding length of 2 cm. The minimal field strength for stability (19) is indicated by corresponding vertical lines.

The bulk charge transport described by Eq. (3) leads to Ohmic behavior and the neutral particle transport due to dielectric pressure leads to a quadratic field dependence condensed in Eq. (2). The formula (26) now combines the effect of charge transport and neutral particle mass transport. It answers the problem raised in Sec. I of how the two pictures can be brought together: the one of incompressible fluids where the velocity is dependent of the area and the one of Ohmic transport where the velocity is only dependent on the electric field.

The resulting total mass current is given in Fig. 4. The current increases basically with the square of the applied field scaled by the bridge length. For additional bulk densities, the mass flow is higher.

B. Comparison with the experiment

To convince the reader of the validity of the velocity formula (26), we compare now with the mass flow and the charge flow measurements. The experimental values of Fig. 4 in Ref. [2] are reported to be 40 mg/s for a bridge of 1 cm length, and a diameter of 2.5 mm for the stationary regime. For this situation, we compare in Fig. 5 the results obtained from Eq. (26) with a pure Ohmic transport using the lowest-order conductivity expression

$$\sigma = \lambda \frac{\rho_c}{eN_A} + \sigma_0, \tag{27}$$

where for clean water the conductivity is σ_0, λ is the molecular conductivity of the solved charge (electrolyte), and N_A is the Avogadro constant; see Table I. We see that our formula (26) leads to a realistic necessary voltage—which was 12.5 kV in the experiment—even if no bulk charge is presented. In contrast, for the Ohmic transport, one has to assume 13 orders of magnitude higher bulk charges to come into the same range. This illustrates the advantage of the model presented here.

Considering the charge transport, we do not expect such big differences between our model and the pure Ohmic picture since there the charged particles matter. To this end, we compare the applied voltage versus bridge length with a constant charge current, as was given in Fig. 6 of Ref. [2].

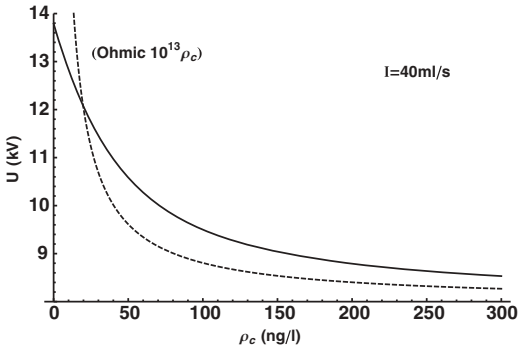

FIG. 5. The necessary applied voltage vs bulk charge densities in order to maintain a mass current of 40 ml/s. Following [2], the length of the bridge was $L = 1$ cm and the diameter was 2.5 mm. The result using the flow expression (26) of the present paper (solid line) is compared to an Ohmic transport (dashed line). For the latter, the bulk charge has been multiplied with 13 orders of magnitude.

In Fig. 6, we compare the result from Eq. (26) with the pure Ohmic transport. We use a bulk charge of 2.3 ng/l. In order to obtain a comparable Ohmic result, we had to multiply the bulk charge with a factor of 3×10^3, which illustrates the difference between our model and the Ohmic transport.

While the difference in charge transport is not very significant provided that the conductivity of water itself varies on the order of three magnitudes, the mass flow of Fig. 5 has shown that our result (26) is superior since it considers the drag of neutral particles due to dielectric pressure together with the charge transport.

Having the current at hand, one estimates the Joule heating easily as

$$\frac{\Delta T}{\Delta t} = \frac{jE}{\rho c_p}. \tag{28}$$

From Fig. 5 of Ref. [2], one sees that the reported increase of 10 K in 30 min would translate into field strengths of 0.7 kV/cm in our calculation. This is much lower than our result. We would obtain here 2–3 orders of magnitude higher

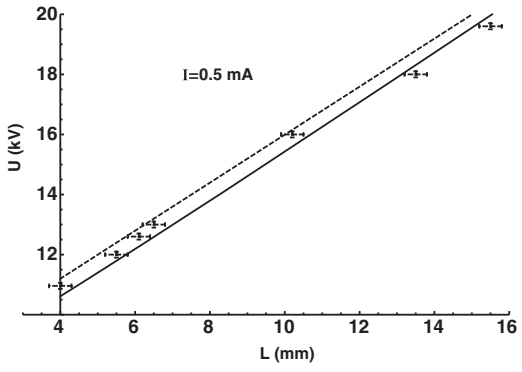

FIG. 6. The necessary applied voltage vs bridge length in order to maintain a charge current of 0.5 mA. The data are from Fig. 6 of Ref. [2]. The result using the flow expression (26) and a bulk charge of 2.3 ng/l (solid line) is compared to an Ohmic transport (dashed line). For the Ohmic transport, the bulk charge has been multiplied with a factor of 3×10^3. The same offset of $U_0 = 8$ kV is used as in the experiments.

heating rates. Please note that the cooling mechanisms such as evaporating and cooling due to water flow are beyond the present consideration. Since these are probably the major cooling effects in the experiments [26], we cannot compare seriously the theoretical heating rate with the experimentally observed ones.

C. Profile of bridge

Let us now calculate the profile of the bridge along the length. We consider to this end the total mass flow of the bridge and neglect the viscous term compared to the kinetic energy (which includes part of the convection term), $\mathbf{u}\nabla\mathbf{u} = \frac{1}{2}\nabla u^2 + \mathrm{curl}\mathbf{u}\times\mathbf{u} \approx \frac{1}{2}\nabla u^2$. Then, one arrives at the Bernoulli equation

$$\rho\frac{v(x)^2}{2} + \rho g f(x) + \sigma_s\left[\frac{1}{R(x)}\right] - \rho_c E x = \rho\frac{v^2}{2} + \sigma_s\frac{1}{R}. \tag{29}$$

Here we have neglected the curvature of the bridge compared to the curvature due to the radius and have compared the position-dependent radius $R(x)$ and velocity $v(x)$ in the bridge with the situation at the beaker, $R(0) = R, v(R) = v$. The Bernoulli equation (29) can be rewritten in terms of the capillary height (1) and the velocity (26) as

$$f(x) - cx = \frac{v^2 - v^2(x)}{2g} + a - \frac{a^2}{2R(x)}, \tag{30}$$

which determines the radius $R(x)$ from the profile of the bridge (15) and the velocity $v(x)$ if we observe the current conservation through an area

$$R(x)^2 v(x) = R^2 v. \tag{31}$$

The results are presented in Figs. 7 and 8. We plot the shape of the bridge, i.e., the radius and the velocity together, with a 3D plot. The case of no bulk charges, which leads to the standard catenary, can be found in Fig. 7, while Fig. 8 shows the situation for extreme bulk charges almost at the stability edge (20). We see a deformation of the catenary due to the applied field. This deformation is observed, e.g., if an additional field is brought near the bridge [2,22]. One sees that the radius is becoming smaller at one end of the bridge accompanied with higher velocities, as is known from falling water pipes [27]. The bulk charge leads to deformations of this profile, which are exaggerated in the plot due to the choice of unequal scales.

Interestingly, such asymmetry is experimentally observed [2], where after 3 min of operation, the asymmetry for the bridge of 0.9 cm length ranges from a diameter of 2.1 to 2.6 mm. This is in agreement with the profile calculated in Fig. 8. Also, the measured asymmetry in the left and right catenary angle [3] in glycerin can be explained with the present model.

D. Dynamical stability

We turn now to the question of the dynamical stability of the flow and consider the motion of water together with the motion of charged particles characterized by the mass m_i and charge e_i. This charge current is given by Ohm's law σE and

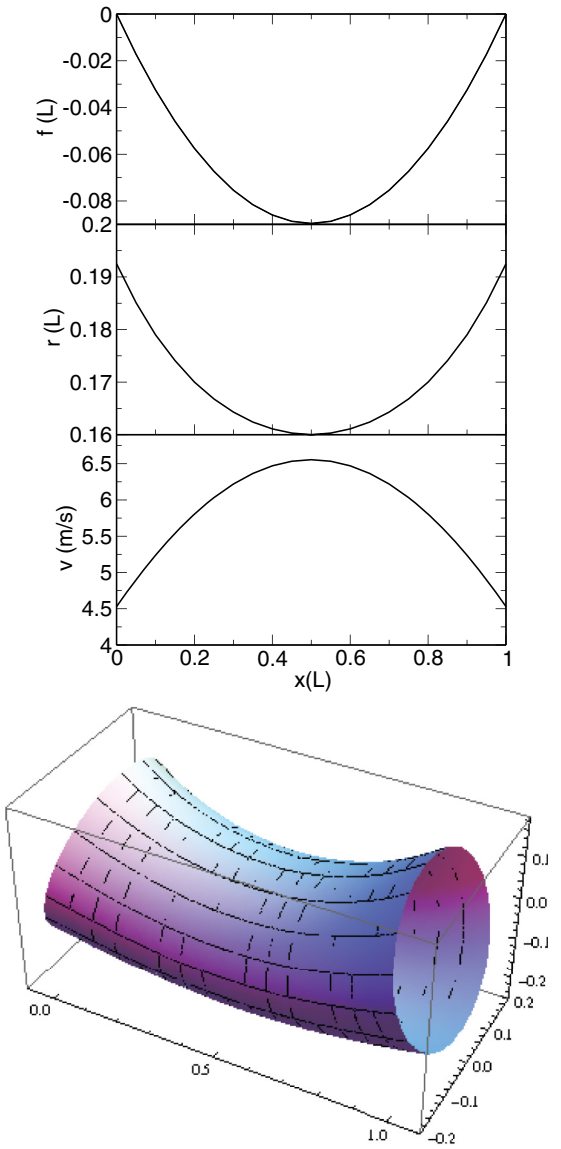

FIG. 7. (Color online) The center-of-mass coordinate (above), the radius (middle), and the velocity (bottom), together with the three-dimensional (3D) plot of the water bridge (in units of L) for no bulk charges, $c = 0$. The parameters are $b = 1.5$ cm and according to Table I. Please note the different length scales in the x and y,z direction.

the corresponding mass current can be written as

$$j_i = \frac{m_i}{e_i} j = x_i\frac{\rho}{\rho_c}\sigma E, \tag{32}$$

where we introduced the mass ratio of the number of charged particles (e.g., NaCl) to the water particles,

$$x_i = \frac{\#_i m_{\mathrm{NaCl}}}{\#_w m_{\mathrm{H_2O}}} = \frac{\rho_c m_i}{\rho e_i}. \tag{33}$$

The mass current of the neutral (water) particles is then

$$j_n = \rho_n v_n = \left(\rho - \frac{m_i}{e_i}\rho_c\right) v_n = (1 - x_i)\rho v_n, \tag{34}$$

such that the total mass current reads

$$\rho v = j_i + j_n = x_i\frac{\rho}{\rho_c}\sigma E + (1 - x_i)\rho v_n. \tag{35}$$

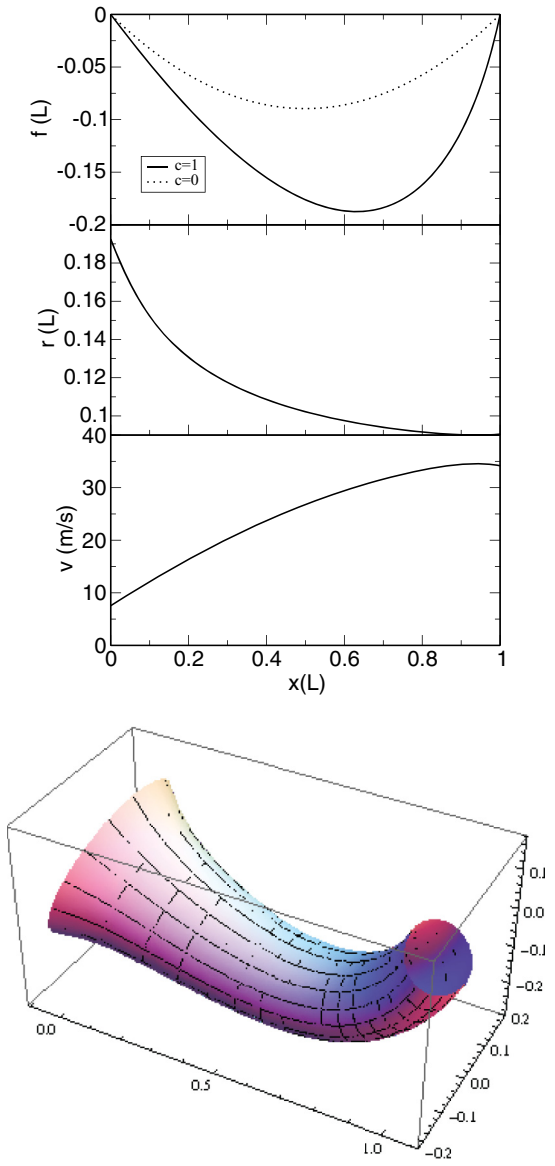

FIG. 8. (Color online) The center-of-mass coordinate (above), the radius (middle), and the velocity (bottom), together with the 3D plot of the water bridge (in units of L) with bulk charges, $c = 1$. The parameters are $b = 1$ cm and according to Table I.

The total current (left side) should be larger than the current only from the charged particles (last term on the right side). However, the velocity of charged particles, $\sigma E/\rho_c$, should be larger than the velocity of the dragged water molecules, v_n, and therefore larger than the mean velocity v of the mass motion. Together with Eq. (26), this is expressed by the inequalities

$$\frac{\sigma E}{\rho_c} > u_0 \left(\frac{b}{L} + c \right) > x_i \frac{\sigma E}{\rho_c}, \tag{36}$$

which gives an upper and lower bound on the possible mass motion created by the drag of particles due to the force on charged particles.

If we now take into account the dependence of the conductivity on the density of the solved ions in water, we can find a condition on possible bulk charges in water to maintain a stable bridge. To this aim, we consider very small

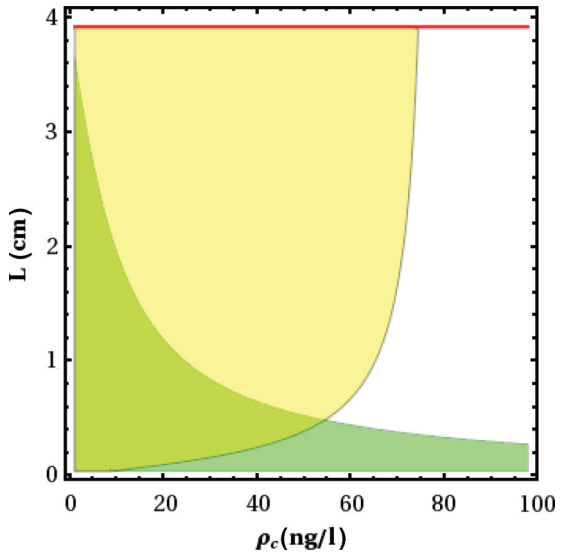

FIG. 9. (Color online) The range of possible water bridges for an electric field of $E = 0.64$ kV/cm. The upper limit is due to the static stability condition (20) and the lower cut is due to the dynamical condition (37). The bulk-charge-free condition is the upper straight line.

charge densities solved in water, which allows one to consider the lowest-order dependence of the conductivity on the bulk charge concentration (27).

Noting the charge-density dependencies of x_i, b, and c via (33), (2), and (3), one obtains from Eq. (36) the dynamical restriction on possible bulk charges,

$$\begin{aligned} \rho_c &\in \rho_1 - \rho_2 \pm \sqrt{(\rho_1 - \rho_2)^2 + \rho_3^2}, \\ \rho_c(1 - 2\rho_2/\rho_i) &> \rho_3^2/\rho_i - 2\rho_1, \end{aligned} \tag{37}$$

with the auxiliary densities

$$\begin{aligned} \rho_1 &= \epsilon_0(\epsilon - 1)\frac{E}{2L}, \quad \rho_2 = \frac{16\eta\lambda}{eN_A a^2}, \\ \rho_3^2 &= \frac{32\eta\sigma_0}{a^2}, \quad \rho_i = \frac{e_i \rho}{m_i}. \end{aligned} \tag{38}$$

The results for NaCl in water (Table I) are plotted in Figs. 9 and 10. The static stability condition (19) gives the upper and charge-density-independent limit in Fig. 10. The static condition (20) with bulk charges leads to the border of maximal densities on the right side, which agrees with Eq. (19) at zero densities, of course. The lower minimal length of the bridge at a given field strength and bulk charge is provided by the dynamical condition (37). For no bulk charge, the possible range of lengths of the bridge starts at zero and is limited by the upper length (19). If there are charges present, then there is a minimal length required to have a stable bridge.

From the 3D plot in Fig. 10, one can see that for finite charges and for fixed bridge lengths, there is a lower and an upper critical field where bridges can only be stable. From the experiments [2], it is seen that the bridge forms jets for fields higher than 15 kV/cm and therefore becomes unstable. With a bridge length of 0.5 cm, this translates into a bulk charge of 4 ng/l, according to our found boundary conditions. This

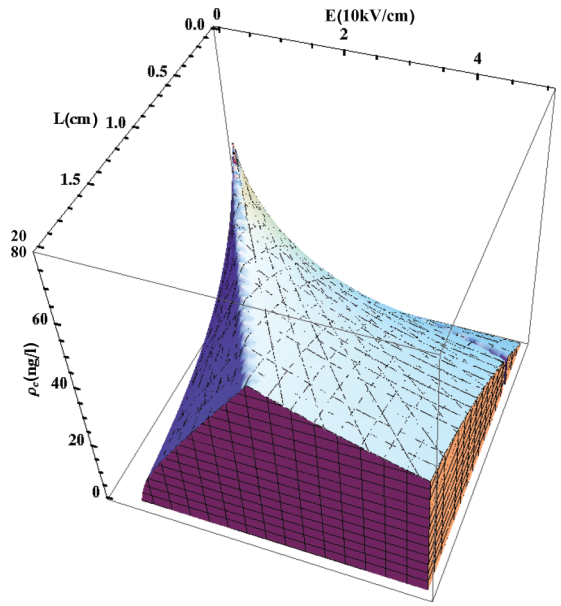

FIG. 10. (Color online) The range of possible water bridges in dependence on the bridge length, the electric field, and the electrolyte bulk charges.

is in agreement with the value needed to reproduce the flow measurements described in Sec. IV B.

V. SUMMARY

The formation of water bridges between two vessels when an electric field is applied has been investigated macroscopically. Electrohydrodynamics is sufficient to describe the phenomenon in agreement with the experimental data. The four necessary parameters, which are constructed from microscopic properties of the charged liquid, are (1) the capillary height, (2) the creeping height, (3) the dimensionless ratio between field and gravitational force density, and (4) the characteristic velocity.

An exact solution has been found of a charged catenary. This leads to a static stability criterion for possible charges in the liquid dependent on the applied field strengths and on the length of the bridge. With no bulk charges present, the maximal bridge length is determined and no minimal length occurs. This changes if bulk charges are present. Then also a minimal length is required. However, only very small concentrations of bulk charges are possible and the bridge is easily destroyed when bulk charges exceed 50 ng/l. As a further result, an asymmetric profile in the diameter along the bridge is obtained, which was observed by asymmetric heating.

For the dynamical consideration, a picture is proposed of dragged liquid particles due to the motion of the charged ones besides the ponderomotoric forces due to the dielectric character of the liquid. The resulting consideration of dynamical stability restricts the possible parameter range of bridge formation. The resulting mass flow combines the charge transport and the neutral mass flow dragged by dielectric pressure and is in agreement with the experimental data.

The presented simple classical theory applies to charged liquids as long as the Reynolds number is so low that laminar flow can be assumed.

ACKNOWLEDGMENTS

The discussions with Bernd Kutschan, who pointed out this interesting effect, and the clarifying comments of Jacob Woisetschläger are gratefully acknowledged. This work was supported by DFG-CNPq Project No. 444BRA-113/57/0-1 and the DAAD-PPP (BMBF) program. The financial support by the Brazilian Ministry of Science and Technology is also acknowledged.

APPENDIX: SOLUTION OF CHARGED CATENARY

Here the derivation of the charged catenary [24] is briefly sketched. We solve the variation problem (14)

$$\int_0^L \mathcal{F}(x)dx \to \text{extr}, \tag{A1}$$

with the functional $\mathcal{F}(x) = \rho g\,[f(x) + b - cx]\sqrt{1 + f'(x)^2}$ and the boundary conditions $f(0) = f(L) = 0$.

It is useful to introduce

$$t(x) = f(x) + b - cx, \tag{A2}$$

such that

$$\mathcal{F}(x) = \rho g\, t(x)\sqrt{1 + [t'(x) + c]^2}. \tag{A3}$$

The corresponding Lagrange equation

$$\frac{d}{dx}\frac{\delta \mathcal{F}}{\delta t'(x)} - \frac{\delta \mathcal{F}}{\delta t(x)} = 0 \tag{A4}$$

possesses a first integral,

$$t'(x)\frac{\delta \mathcal{F}}{\delta t'(x)} - \mathcal{F} = \text{const} = -\xi\sqrt{1 + c^2}, \tag{A5}$$

where we introduced the first integration constant ξ in a convenient way.

The resulting differential equation

$$t(\bar{x})[ct'(\bar{x}) + 1] = \xi\sqrt{t'(\bar{x})^2 + [ct'(\bar{x}) + 1]^2} \tag{A6}$$

with $\bar{x} = x(1 + c^2)$ is solved in an implicit way,

$$t(\bar{x}) = \xi \cosh\left\{\frac{1}{\xi}\left[\bar{x} + ct(\bar{x}) - cb + \frac{L}{2}d\right]\right\}, \tag{A7}$$

with a second integration constant d. The profile is therefore given by the implicit equation

$$f(x) = cx - b + \xi \cosh\left\{\frac{1}{\xi}\left[x + cf(x) + \frac{L}{2}d\right]\right\}. \tag{A8}$$

The boundary condition $f(0) = 0$ leads to the determination of the integration constant

$$d = 2\frac{\xi}{L}\text{arcosh}\left(\frac{b}{\xi}\right) \tag{A9}$$

in terms of the yet unknown ξ constant. The solution (A8) can be written with the help of Eq. (A9) as

$$f(x) = cx + \xi\left\{\cosh\left[\frac{x + cf(x)}{\xi} - \frac{Ld}{2\xi}\right] - \cosh\left(\frac{Ld}{2\xi}\right)\right\}. \tag{A10}$$

The boundary condition $f(L) = 0$ leads to the determination of the remaining constant ξ to be the solution of the equation

$$c = -\frac{2\xi}{L}\sinh\frac{L}{2\xi}\left(\frac{b}{\xi}\sinh\frac{L}{2\xi} - \sqrt{\frac{b^2}{\xi^2}-1}\cosh\frac{L}{2\xi}\right). \tag{A11}$$

Finally, we can rewrite the implicit solution (A10) in parametric form. Therefore, we choose as the parameter $t = x + cf(x)$, which runs obviously through the interval $t \in (0, L)$, and we obtain the solution (15)

$$f(t) = \frac{1}{1+c^2}\left\{c\,t+\xi\left[\cosh\left(\frac{t}{\xi}-\frac{Ld}{2\xi}\right)-\cosh\left(\frac{Ld}{2\xi}\right)\right]\right\},$$
$$x(t) = t - cf(t), \quad t \in (0, L). \tag{A12}$$

[1] W. G. Armstrong, *The Electrical Engineer* (Newcastle Lit. and Phil. Soc., Newcastle upon Tyne, UK, 1893), pp. 154 and 155.
[2] J. Woisetschlager, K. Gatterer, and E. C. Fuchs, Exp. Fluids **48**, 121 (2010).
[3] A. G. Marin and D. Lohse, Phys. Fluids **22**, 122104 (2010).
[4] G. M. Sacha, A. Verdaguer, and M. Salmeron, J. Phys. Chem. B **110**, 14870 (2006).
[5] J. M. Oh, S. H. Ko, and K. H. Kang, Phys. Fluids **22**, 032002 (2010).
[6] A. Garcia-Martin and R. Garcia, Appl. Phys. Lett. **88**, 123115 (2006).
[7] S. Gómez-Monivas, J. J. Sáenz, M. Calleja, and R. García, Phys. Rev. Lett. **91**, 056101 (2003).
[8] T. Cramer, F. Zerbetto, and R. Garcia, Langmuir **24**, 6116 (2008).
[9] S. Chen, X. Huang, N. F. A. van der Vegt, W. Wen, and P. Sheng, Phys. Rev. Lett. **105**, 046001 (2010).
[10] T. M. Squires and S. R. Quake, Rev. Mod. Phys. **77**, 977 (2005).
[11] A. M. Ganancalvo, J. Fluid Mech. **335**, 165 (1997).
[12] M. Gamero-Castano, J. Fluid Mech. **662**, 493 (2010).
[13] F. Higuera, Phys. Fluids **22**, 112107 (2010).
[14] J. Eggers, Phys. Rev. Lett. **71**, 3458 (1993).
[15] J. Eggers, Rev. Mod. Phys. **69**, 865 (1997).
[16] F. Saija, F. Aliotta, M. E. Fontanella, M. Pochylski, G. Salvato, C. Vasi, and R. C. Ponterio, J. Chem. Phys. **133**, 081104 (2010).
[17] J. R. Melcher and G. I. Taylor, Ann. Rev. Fluid Mech. **1**, 111 (1969).
[18] L. D. Landau and E. M. Lifschitz, *Lehrbuch der Theoretischen Physik: Elektrodynamik der Kontinua* (Akademie-Verlag, Berlin, 1990), Vol. VIII.
[19] A. Ramos, H. Morgan, N. G. Green, and A. Castellanos, J. Phys. D: Appl. Phys. **31**, 2338 (1998).
[20] A. Widom, J. Swain, J. Silverberg, S. Sivasubramanian, and Y. N. Srivastava, Phys. Rev. E **80**, 016301 (2009).
[21] L. Giuliani, E. D'emilia, A. Lisi, S. Grimaldi, A. Foletti, and E. Del Giudice, Neural Network World **19**, 393 (2009).
[22] E. C. Fuchs, J. Woisetschlager, K. Gatterer, E. Maier, R. Pecnik, G. Holler, and H. Eisenkolbl, J. Phys. D: Appl. Phys. **40**, 6112 (2007).
[23] D. E. Moulton and J. A. Pelesko, Siam J. Appl. Math. **70**, 212 (2009).
[24] K. Morawetz, AIP Advances **2**, 022146 (2012).
[25] D. S. Chandrasekharaiah, *Continuum Mechanics* (Academic, Boston, 1994).
[26] J. Woisetschlager (private communication).
[27] M. J. Hancock and J. W. Bush, J. Fluid Mech. **466**, 285 (2002).